RSC Advances

PAPER

View Article Online
View Journal | View Issue

Cite this: *RSC Adv.*, 2024, **14**, 26494

An efficient and simple approach for synthesizing indazole compounds using palladium-catalyzed Suzuki–Miyaura cross-coupling†

Bandaru Gopi and Vijayaparthasarathi Vijayakumar *

A series of indazole derivatives (**6a–6i** and **7a–7i**) has been synthesized using Suzuki Miyaura cross-coupling with a palladium catalyst from readily available starting materials. An efficient and reliable methodology was employed for the synthesis, and the compounds were thoroughly characterized using ^{1}H NMR, ^{13}C NMR, FT-IR, and HRMS analysis to confirm their structural integrity and purity. Density function theory (DFT) computation identified four compounds (**6g**, **6h**, **7g**, and **7h**) with significant energy band gaps. Additionally, the molecular electrostatic potential study highlighted the distinct electrical characteristics of these indazole molecules. Subsequent molecular docking investigations were carried out using the AUTODOCK method with two separate protein data bank (PDB) structures (6FEW, 4WA9) involved in renal cancer pathways. The results showed that eight substances PDB: 6FEW (**6g**, **6h**, **7g**, and **7h**) and PDB: 4WA9 (**6a**, **6c**, and **7c**, **7g**) had the highest binding energies, indicating their potential as therapeutic agents for treating kidney cancer.

Received 25th June 2024
Accepted 15th August 2024

DOI: 10.1039/d4ra04633a

rsc.li/rsc-advances

Introduction

Indazoles are important nitrogen-containing heterocyclic compounds; consisting of a ten-electron aromatic molecule with a pyrazole and benzene ring.[1] Direct radical addition is effective at the C3 position of indazole such as alkylation, arylation, benzylation, amination, sulfonation, trifluoromethylation, and phosphorylation.[2] Indazole is a suitable pharmacophore with distinct physiological and pharmacological activities and it can be used as a bio-isosteric alternative for other heterocycle structures such as indole and benzimidazole.[3] Numerous natural and synthetic medicinal chemicals are produced from indazoles, including axitinib lonidamine, granisetron, and benzydamine (Fig. 1). Axitinib is a powerful tyrosine kinase inhibitor used to treat renal cell cancer. Lonidamine is a hexokinase inhibitor, commonly used as a chemotherapeutic drug renowned for its antitumor characteristics. Granisetron is a specific 5-HT-3 antagonist, is used as an antiemetic in cancer radiotherapy. Benzydamine is also used for its anti-inflammatory and analgesic properties.[4] The *in vitro* and *in vivo* anti-cancer effectiveness of indazole compounds produced as kinase inhibitors has been intensively studied. For example, the multikinase inhibitor pazopanib (Fig. 1), the c-met inhibitor merestinib (Fig. 1), and the tropomyosin receptor kinase/proto-oncogene tyrosine-protein kinase ROS1/anaplastic lymphoma kinase inhibitor entrectinib (Fig. 1) are all authorized for the treatment of various cancer types.[5–8] Cancer is characterized as unexpected or aberrant cell growth (neoplasia) produced by a variety of metabolic abnormalities in cell physiology. Metabolic problems have existed for many decades, and scientists are working to create perfect management or entire irradiation therapy remains a difficulty and is still being investigated today.[9] Globocan, the worldwide cancer research agency, estimated 19.3 million new cancer cases and 10 million cancer deaths in 2020. Cancer is one of the leading causes of mortality globally. Females account for more breast cancer patients (11.7%), whereas males account for the bulk of lung cancer cases (18%). Other common cancers include colorectal (9.4%), liver (8.3%), and prostate (7.3%). In 2020, a high number of new cases of kidney cancer were projected. Renal cell carcinoma is responsible for 90% of all kidney cancer occurrences globally. Therefore there is a need to develop novel anticancer medications with low side effects and good bioavailability.[10,11] Heterocyclic organic chemistry has spurred interest in its potential biological, agricultural, and industrial applications. Indazole heterocycle molecule is a functional substituent and scaffold that has been investigated for its potential as a kinase inhibitor in cancer treatment. It possesses pharmacological properties[12] such as including anti-tumor,[13] anti-HIV,[14] anti-inflammatory,[15] anti-depressant,[16] anti-leukemia,[17] anti-convulsant,[18] anti-arthritic,[19] anthelmintic,[20] anti-diabetic,[21] and antipyretic. Due to its effectiveness, many anticancer drugs utilize indazole as a key structural component.[22] The Suzuki–Miyaura cross-coupling technique is used to synthesize indazole compounds, which is a highly effective

Department of Chemistry, School of Advanced Sciences, Vellore Institute of Technology, Vellore, 632014, India. E-mail: kvpsvijayakumar@gmail.com; vvijayakumar@vit.ac.in

† Electronic supplementary information (ESI) available. See DOI: https://doi.org/10.1039/d4ra04633a

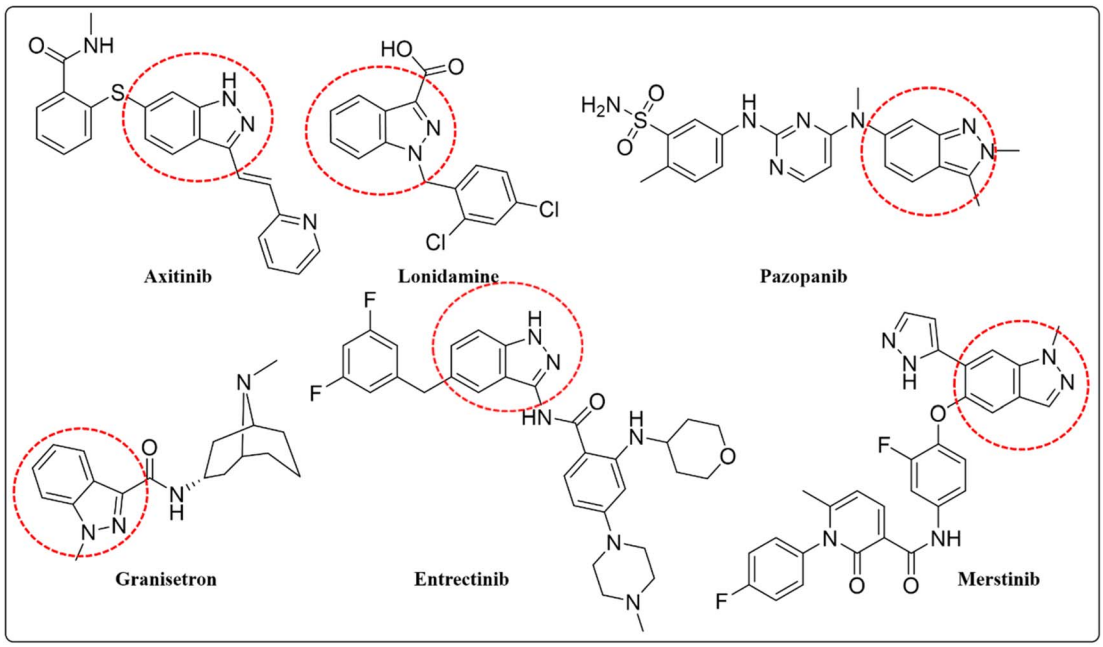

Fig. 1 Commercially available indazole drugs.

method of forming the C–C bond. This technique involves, reacting an aryl halide with organoboronic acid using palladium as a catalyst. The synthesis process uses palladium (Pd) precursors (salts).[23] The most efficient method of creating new indazole compounds is by using the Pd (0) to Pd(II) cycle. This involves treating an aryl halide with Pd (0) in an oxidative manner to create a Pd(II) intermediate. This intermediate is then *trans*-metalated and withdrawn reductively to produce the active Pd (0) and the corresponding product.[24]

Results and discussion

The widely accessible desired target molecules *N*-(4-bromophenyl)-1-butyl-1*H*-indazole-3-carboxamide (**6**) and *N*-(3-bromophenyl)-1-butyl-1*H*-indazole-3-carboxamide (**7**) were synthesized using acid amide cross-coupling. The synthesis involved employing HATU (hexafluorophosphate azabenzotriazole tetramethyl uronium) amide coupling reagent and DIPEA (*N*,*N*-diisopropylethylamine) in DMF at room temperature for 12–16 hours. After the reaction was completed, as confirmed by TLC using 20% ethyl acetate/hexane as eluent, the reaction mixture was quenched with ice-cold water to precipitate solid, which was then dried under a hot-air oven at 60–70 °C for 2 hours to obtain off-white solids of (**6**) and (**7**). Suzuki–Miyaura coupling of **6** and **7** with various organoboronic acids was employed to develop novel indazole compounds (Fig. 2). Optimization studies are detailed in Table 1. The reaction involved using Bromo-indazole carboxamide (0.404 mmol), boronic acid (1.212 mmol), and K_2CO_3 (1.212 mmol) as bases in $PdCl_2(dppf)\cdot(DCM)$ (0.020 mmol), water, and 1,4-dioxane/water were used as solvents at 100 °C for 12 hours. TLC (20% ethyl acetate/hexane) confirmed the completion of the reaction, and the reaction mixture was filtered through a Celite pad under a high vacuum. The filtrate was then dissolved in ethyl acetate, and extracted (2 × 50 mL) with water (50 mL). The organic layer was dried over sodium sulphate under decreased pressure to produce crude, which was refined using column chromatography (R_f = 0.5, 15% ethyl acetate/hexane). This method was used to generate all of the derivatives given in (Fig. 3), and (Fig. 4) depicts a plausible mechanism for the Suzuki–Miyaura coupling.

DFT studies

Theoretical investigation was conducted using density functional theory (DFT) calculations, and indazole derivatives were modelled in the Gaussian 6.1 software using the base set B3LYP/6-31G(d,p). The Frontier Molecular Orbital (FMO) is a type of molecular orbital described in ESI.†[25–27] The HOMO (Highest Occupied Molecular Orbital) and LUMO (Lowest Unoccupied Molecular Orbital) were calculated using the DFT technique. The E_{HOMO} (HOMO energy) values indicate that the molecule donates electrons to the acceptor molecule, while the E_{LUMO} (LUMO energy) values suggest that the molecule readily accepts electrons from the donor molecule.[28] All derivatives were calculated using the DFT technique. The four compounds with the highest energy values are **6g**, **6h**, **7g**, and **7h**, and (Fig. 5) displays the frontier orbital (FMO) of these compounds. To calculate the energy difference between HOMO and LUMO values, the formula $\Delta E = E_{LUMO} - E_{HOMO}$ can be applied.[29] The ESI† contains estimated DFT values for other indazole derivatives. HOMO–LUMO energies were used to calculate electronic parameters, including ionization potential (I), electron affinity (A), and global descriptors such as absolute electronegativity (χ), chemical potential (μ), hardness (η), softness (S), and electrophilicity index (ω) of electron-donating power (ω^-) and electron-

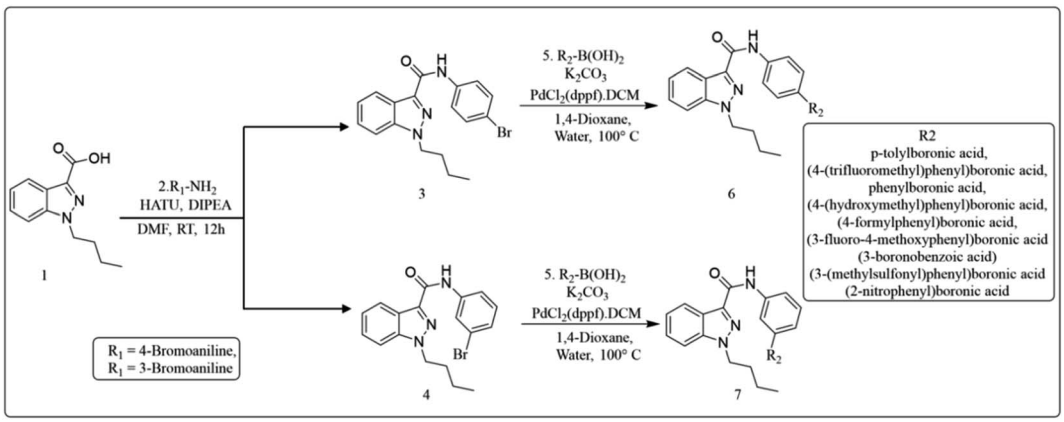

Fig. 2 Procedure for preparation of indazole derivatives by Suzuki reaction.

Table 1 Optimization studies

Entry	Catalyst	Base	Solvent	Yield %
1	$PdCl_2(dppf)\cdot DCM$	K_2CO_3	THF/water	35%
2	$PdCl_2(dppf)\cdot DCM$	Cs_2CO_3	THF/water	30%
3	$PdCl_2(dppf)\cdot DCM$	Na_2CO_3	THF/water	40%
4	$PdCl_2(dppf)\cdot DCM$	DIPEA	THF/water	Trace
5	$PdCl_2(dppf)\cdot DCM$	K_2CO_3	Toluene/water	30%
6	$PdCl_2(dppf)\cdot DCM$	Cs_2CO_3	Toluene/water	25%
7	$PdCl_2(dppf)\cdot DCM$	Na_2CO_3	Toluene/water	30%
8	$PdCl_2(dppf)\cdot DCM$	DIPEA	Toluene/water	Trace
9	$PdCl_2(dppf)\cdot DCM$	K_2CO_3	1,4-Dioxane/water	94.4%
10	$PdCl_2(dppf)\cdot DCM$	Cs_2CO_3	1,4-Dioxane/water	60%
11	$PdCl_2(dppf)\cdot DCM$	Na_2CO_3	1,4-Dioxane/water	65%
12	$PdCl_2(dppf)\cdot DCM$	DIPEA	1,4-Dioxane/water	Trace
13	$PdCl_2(dppf)\cdot DCM$	K_2CO_3	DMF/water	27%
14	$PdCl_2(dppf)\cdot DCM$	Cs_2CO_3	DMF/water	22%
15	$PdCl_2(dppf)\cdot DCM$	Na_2CO_3	DMF/water	30%
16	$PdCl_2(dppf)\cdot DCM$	DIPEA	DMF/water	Trace

accepting power (ω^+),[30,31] at the 6-31G(d,p) level, with the parameters listed in Table 2. The ESI† demonstrates the electronic characteristics of the indazole compounds.

Molecular electrostatic potential

The molecular electrostatic potential (MEP) can be used to predict a molecule's reactivity to nucleophilic and electrophilic attacks. It is based on the molecule's electrical properties such as dipole moment, electronegativity, atomic charges, and so on. MEP is particularly useful for understanding electrophilic and nucleophilic reactions and hydrogen bonding. In this study, the MEP surface analysis of the compound was performed using DFT calculations with the optimized structure and the B3LYP/6-31G(d,p) basis set.[32–34] The analysis revealed the electrophilic (positive) and nucleophilic (negative) attack regions on molecules **6g**, **6h**, **7g**, and **7h** (Fig. 6). shows the electron densities of **6g** (−8.284e negative and 8.284e positive site), **6h** (−7.664e negative and 7.664e positive site), **7g** (−8.117e negative site and +8.117e positive site), and **7h** (−7.683e negative site and 7.683e positive site), representing the compounds' mapped

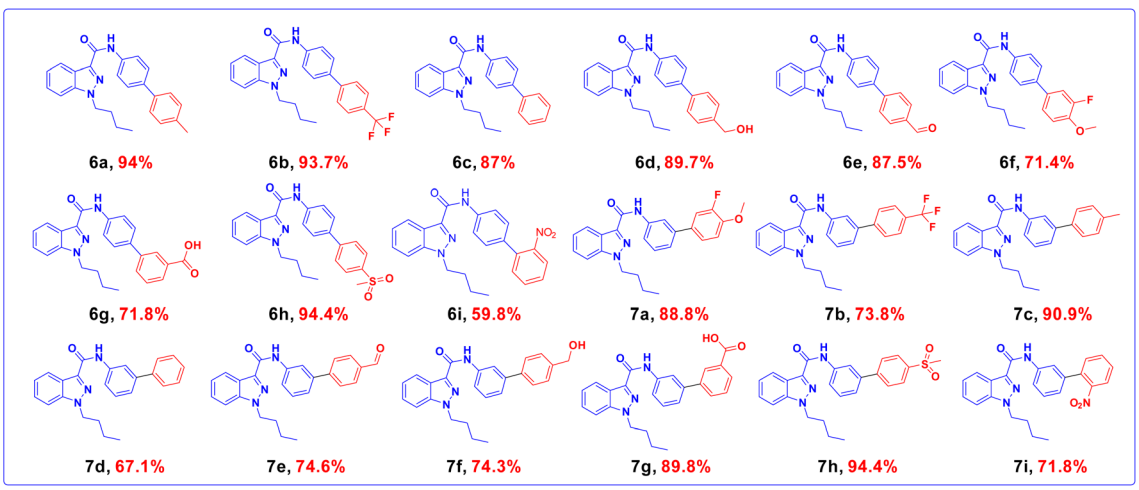

Fig. 3 Indazole derivatives from **6a–6i**, and **7a–7i**.

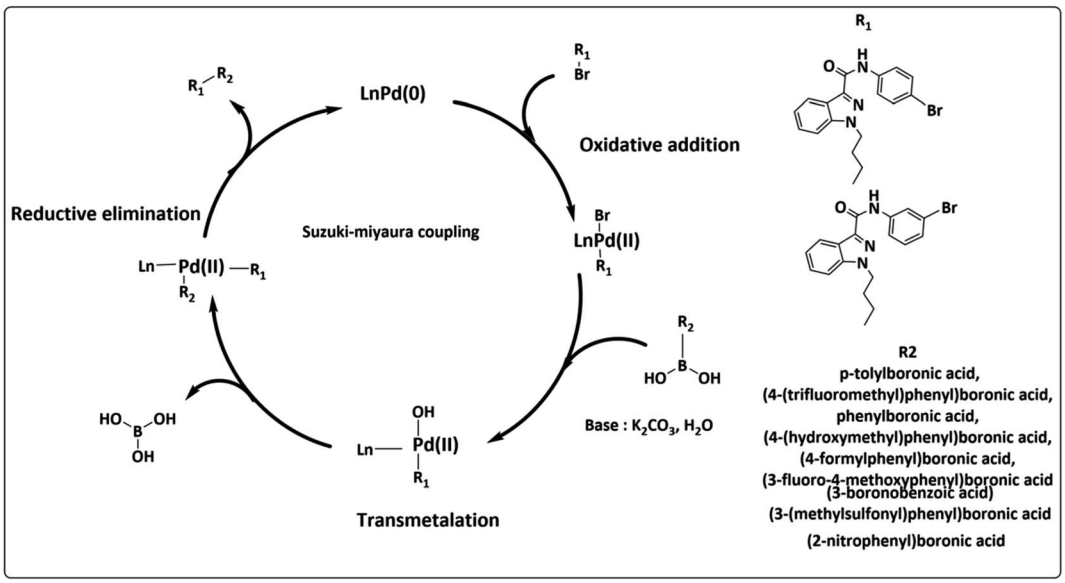

Fig. 4 Plausible mechanism for Suzuki–Miyaura coupling.

electrostatic potential surface. Different colours represent different electrostatic potential levels, as well as zones of positive, negative, and neutral potential. Blue signifies an electrophilic site, red symbolizes a nucleophilic site, and green indicates an area with a neutral electrostatic potential. Nucleophilic sites are found on oxygen, nitrogen, and sulfur atoms, while electrophilic sites are on hydrogen atoms. As a result, nucleophilic and electrophilic molecules tend to prefer locations with lower electronegative potential and higher electrostatic potential.

Molecular docking

The literature has identified entrectinib, pazopanib, and axitinib as the three most commonly available indazole-containing medicines with potent anti-renal cancer activity. To explore the efficacy of these newly synthesised molecules, we utilized axitinib-related PDB 4WA9 and another renal cancer-related PDB 6few. To explore the binding interaction of the indazole derivative, we conducted *in silico* studies. Auto Dock tools (version 1.5.6) were used to generate receptor grid maps for the docking investigation.[35] We searched the protein databank for the protein crystallographic structures (PDB: 4WA9 and PDB: 6few) and utilized them in our studies (PDB: 4WA9, the crystal structure of human abl1 wild-type kinase domain in association with axitinib and PDB: 6FEW, DDR1: 2-[8-(1*H*-idazole-5-carbonyl) (4-oxo-1phenyl-1,3,8-triazspiro [4.5] decan-3-yl]-*N*-methylacetamide) (Fig. 7). The protein was synthesized using the Bioviva Discovery Studio software program (**http://**

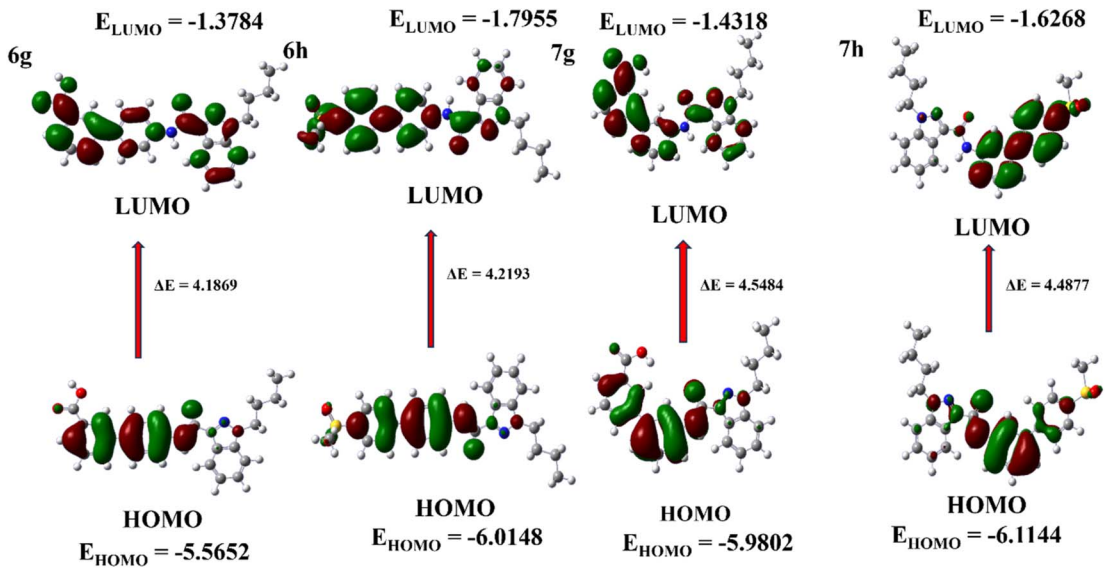

Fig. 5 Frontier molecular orbitals and HOMO–LUMO energy level diagram of **6g**, **6h**, **7g**, and **7h**.

Table 2 Electronic parameters of indazole derivatives for **6g**, **6h**, and **7g**, **7h**[a]

S. no.	HOMO (eV)	LUMO (eV)	$\Delta E = E_{LUMO} - E_{HOMO}$ (eV)	$I = -EHOMO$ (eV)	$A = -E_{LUMO}$ (eV)	$\chi = (I+A)/2$ (eV)	$\mu = -\chi$ (eV)	$\eta = (I-A)/2$ (eV)	$S = 1/\eta$ (eV)	$\omega = \mu^2/2\,\eta$	$\omega^- = (3I+A)^2/16(I-A)$	$\omega^+ = (I+3A)^2/16(I-A)$
6g	−5.5652	−1.3784	4.1869	5.5652	1.3784	3.4718	−3.4718	2.0934	0.4777	12.6165	85.4837	24.6230
6h	−6.0148	−1.7955	4.2193	6.0148	1.7955	3.9051	−3.9051	2.1096	0.4740	16.0862	103.7999	34.2789
7g	−5.9802	−1.4318	4.5484	5.9802	1.4318	3.7060	−3.7060	2.2742	0.4397	15.6177	106.6871	30.0165
7h	−6.1144	−1.6268	4.4877	6.1144	1.6268	3.8706	−3.8706	2.2438	0.4457	16.8079	111.8555	33.9051

[a] HOMO = highest occupied molecular orbital, LUMO = lowest unoccupied molecular orbital, I = ionisation, A = electron affinity, χ = electronegativity, μ = potential efficiency, η = hardness, S = softness, ω = electrophilicity, ω^- = e donating power, ω^+ = e accepting power.

www.discover.3ds.com/discovery-studio-visualizer-download).[36] Following that, we eliminated the protein's water molecules, binding ligands, and other components. After removing water molecules, binding ligands, and other components, the atoms were filled by polar hydrogen atoms and allocated Gasteiger charges within the receptor. The ligand was then charged with Gasteiger in the Avogadro program and the corresponding protein structure was used as an input file for the auto grid method after the Kollman charges were assigned [maps were created using auto grid with 0.375 Å spacing between grid points for each atom type in the ligand,[37] the grid box's center was set to $x = 9.47003$, $y = 154.99967$, and $z = 35.72421$. The active site box has dimensions of 40.40-40 (ref. 38)]. Flexible ligand docking was performed on the selected molecules. Each docked system received ten cycles of the Auto Dock search using the Lamarckian genetic method. After doing all of the derivative docking experiments, we compared the results to the axitinib-related PDB: 4wa9 and the renal cancer-related PDB: 6few. All of the derivatives showed almost identical binding energies displayed in Table 3, (1) final intermolecular energy + vander Waal + H-bond + desolv energy, (2) final total internal energy, (3) torsional free energy, and (4) unbound system's energy, which were obtained using the formula [(1) + (2) + (3) − (4)] in kcal mol^{-1}. Furthermore, these docking studies illustrated the interaction of amino acids, using the 2D diagram-related structure displayed in Fig. 8. The Discovery Studio visualizer was used to analyze 2D ligand–receptor interactions and all derivatives was highlighted in the ESI.†

Conclusions

In summary, the study has discovered a new method of combining indazole derivatives and various boronic acids using the Suzuki–Miyaura coupling mechanism. The synthesized

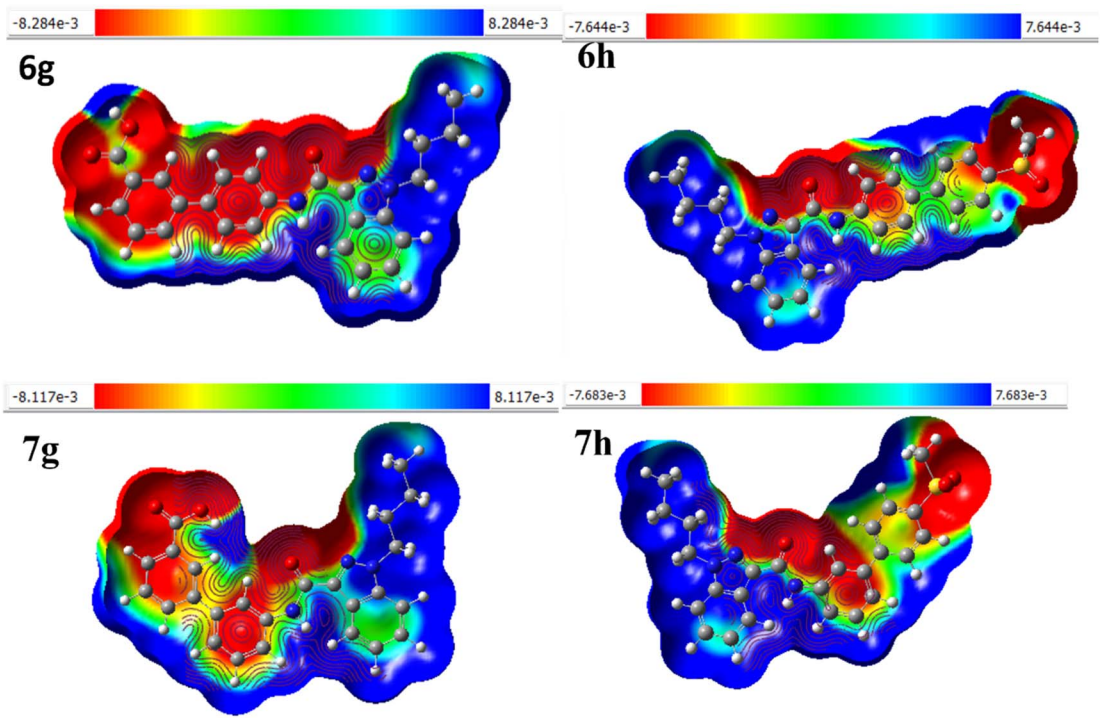

Fig. 6 The molecular electrostatic potential surface of **6g**, **6h**, **7g**, and **7h**.

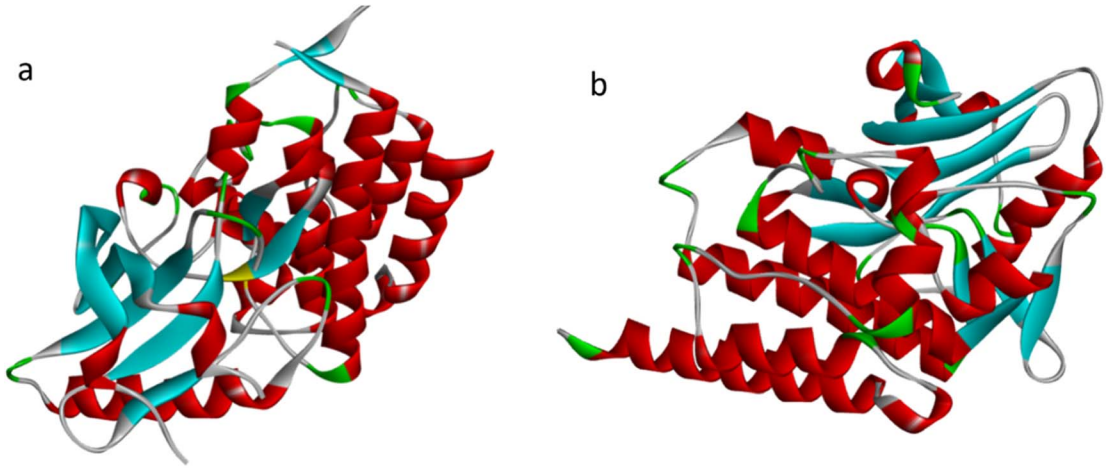

Fig. 7 (a) PDB: 6FEW, DDR1, 2-[8-(1*H*-idazole-5-carbonyl)-4-oxo-1phenyl-1,3,8-triazspiro[4.5]decan-3-yl]-*N*-methylacetamide (b) PDB: 4WA9, the crystal structure of human abl1 wild-type kinase domain in complex with axitinib.

derivatives were thoroughly validated using FT-IR, HRMS, and ^{1}H and ^{13}C NMR spectroscopy. Using Density Functional Theory (DFT) calculations, four compounds with high energy states were identified and analysed through molecular electrostatic potential surface investigations. Docking studies were conducted using AutoDock software version 1.5.6 and Protein Data Bank entries 4WA9 and 6FEW. The results showed that compounds (**6g**, **6h**, and **7h**, **7i**) and (**6a**, **6c**, and **7c**, **7g**) exhibited strong binding affinities.

Experimental section

All the necessary chemicals and solvents used in the experiment were purchased from commercially available chemical suppliers and used as received without further purification. The solvents DMF and 1,4-dioxane were obtained from Finar chemical suppliers, while the remaining chemicals were purchased from Avra Chemicals and Sigma-Aldrich. All the reactions were carried out in round bottom flasks. The infrared absorption spectra were recorded on an affinity-1 (4000–200 cm^{-1}). The 1-butyl-1*H*-indazole-3-carboxamide was prepared according to the reported protocols. The ^{1}H-NMR and ^{13}C-NMR spectra were recorded at room temperature on a Bruker Avance III (400 MHz) spectrometer using $CDCl_3$ as a solvent and TMS as an internal standard and are referred to as the residual solvent signal $CDCl_3$: (7.26) for ^{1}H and (77.16) for ^{13}C NMR: dimethyl sulfoxide-d_6 (2.50) for ^{1}H and (39.50) for ^{13}C NMR: chemical shift (δ) is given in ppm and coupling constant (J) were measured in Hz. The following abbreviations are used: s-singlet, d-doublet, dd-doublet of doublet, t-triplet, td-triplet of doublet, dt-doublet of triplet, q-quartet, qd-quartet of doublet, qn-quintet, br-broad, m-multiplet. HRMS ESI-MS was recorded using Xeo G2 XS OT of (water) and values are given m/z. Column chromatography uses a glass column of silica gel (100–200 mesh). Analytical TLC was carried out on Macherey-Nagel 60 F245 aluminium-backed silica gel plates.

General procedure for the synthesis of 3 and 4

To a stirred solution of 1-butyl-1*H*-indazole-3-carboxylic acid (250 mg, 1.146 mmol) was dissolved in DMF (10 mL), HATU (2 equivalents), and DIPEA (3 equivalents) was added to the reaction mixture, then commercial amines (2 equivalents) were added. The reaction mixture was stirred at room temperature

Table 3 Docking results in terms of binding energy (kcal mol^{-1}), most efficient anticancer (renal cancer) **6a**, **6c**, **6g**, **6h**, and **7c**, **7g**, **7h**,**7i** derivatives

Entry	Receptor	(1) Final intermolecular energy + van der Waal + H-bond + desolv energy (kcal mol^{-1})	(2) Final total internal energy (kcal mol^{-1})	(3) Torsional free energy (kcal mol^{-1})	(4) Unbound system's energy (kcal mol^{-1})	(ΔG) binding energy = [(1) + (2) + (3) − (4)] (kcal mol^{-1})
6a	4wa9	−12.21	−1.64	+1.79	−1.89	−10.42
6c	4wa9	−10.87	−1.87	+1.79	−1.87	−9.08
7c	4wa9	−12.06	−0.98	+1.79	−0.98	−10.27
7g	4wa9	−12.95	−1.01	+2.39	−1.01	−10.57
6g	6few	−14.40	−1.71	+2.39	−1.71	−12.02
6h	6few	−13.88	−1.89	+2.09	−1.89	−11.79
7h	6few	−15.28	−1.48	+2.09	−1.48	−13.19
7i	6few	−15.08	−2.14	+2.09	−2.14	−12.99

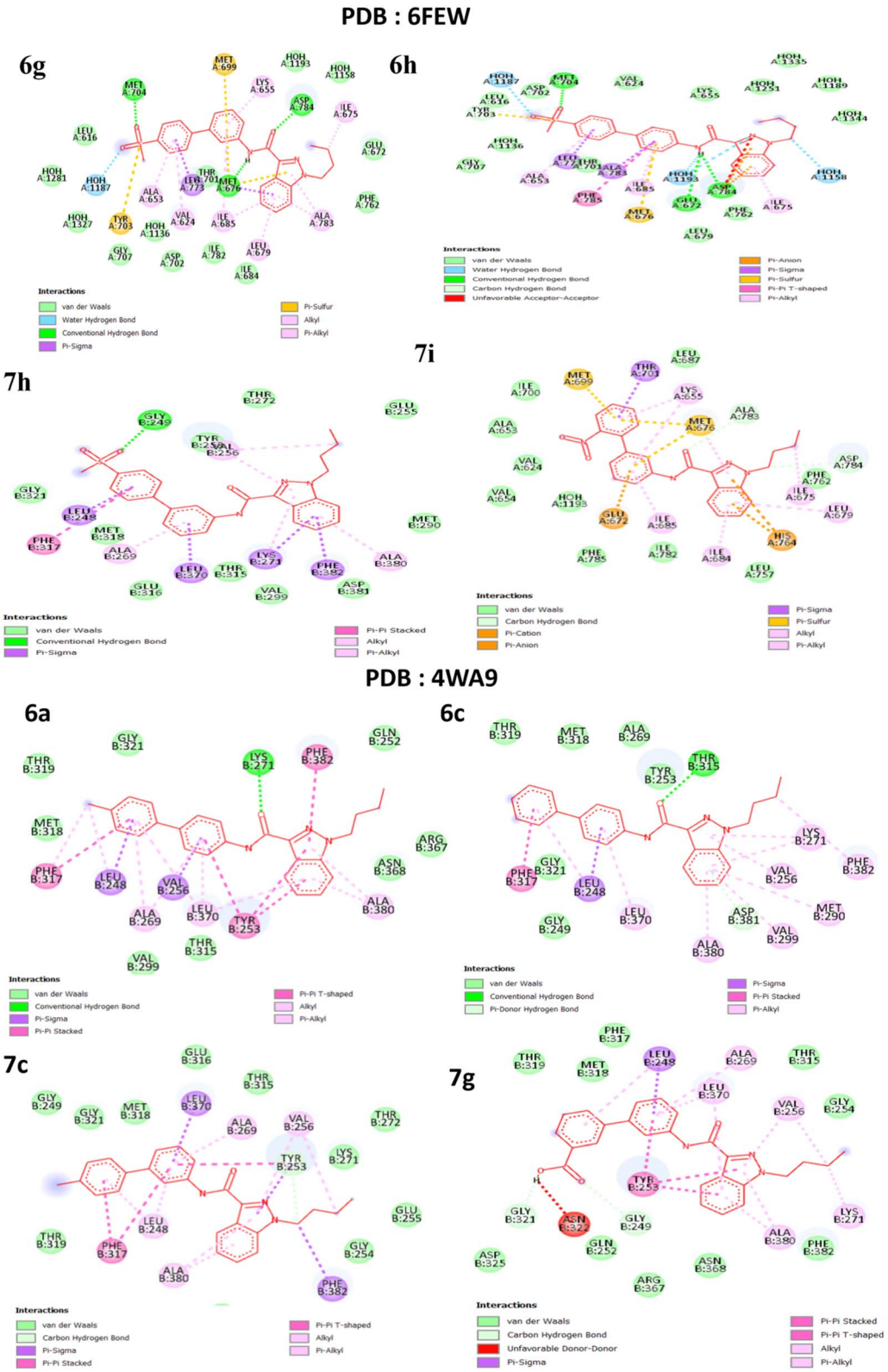

Fig. 8 2D predicted binding mode of compounds PDB: 6FEW (**6g**, **6h** and **7h**, **7i**) and PDB: 4wa9 (**6a**, **6c**, and **7c**, **7g**).

for 8–16 hours. After completion of the reaction, the resultant reaction mixture was poured into ice-cold water, and solid precipitated and filtered through the Buchner funnel under a high vacuum dried to obtain pure compound **3** and **4.**

General procedure for Suzuki reaction (6a–6i, 7a–7i)

To a stirred solution of *N*-(3-bromophenyl)-1-butyl-1*H*-indazole-3-carboxamide (150 mg) was dissolved in 1,4-dioxane/water (6/2 mL), K_2CO_3 (3 eq.), and Pd(dppf)Cl_2·DCM (0.05 eq.) was added

to the reaction mixture, and commercial boronic acids (3 eq.) were added. The reaction mixture was stirred at room temperature for 8–12 hours. After completion of the reaction, the resultant reaction mixture was filtered through a Celite pad with a Buchner funnel under a high vacuum, the filtrate was extracted with water and ethyl acetate (4 × 20 mL). The organic layer was dried with anhydrous sodium sulphate and the solvent was removed under reduced pressure to afford crude product. The crude was purified by silica gel chromatography to obtain a pure compound (**6a–6i**, **7a–7i**).

Characterization of indazole derivatives (3, 4) and (6a–6i, 7a–7i)

1-Butyl-1*H*-indazole-3-carboxylic acid to *N*-(4-bromophenyl)-1-butyl-1*H*-indazole-3-carboxamide (3). Appearance: brown solid (melting point = 96–99 °C, yield = 82.5%, weight = 210.6 mg). ^{1}H NMR [400 MHz, DMSO-d$_6$]: δ 10.41 (s, 1H), 8.23 (d, J = 8.40 Hz, 1H), 7.90 (d, J = 8.80 Hz, 2H), 7.83 (d, J = 8.40 Hz, 1H), 7.55–7.52 (m, 3H), 7.32 (t, J = 7.60 Hz, 1H), 4.55 (t, J = 7.20 Hz, 2H), 1.90 (q, J = 7.20 Hz, 2H), 1.34–1.32 (m, 2H), 0.91 (t, J = 7.20 Hz, 3H). ^{13}C NMR [100 MHz, DMSO-d$_6$]: δ 161.16, 141.18, 138.68, 137.23, 131.82, 127.24, 123.18, 122.74, 122.18, 111.04, 55.37, 31.99, 19.92, 14.01. IR STRECHING (cm^{-1}): 3272 (N–H), 1655 (C=O). HRMS (ESI) m/z: [M + H] calculated $C_{18}H_{18}BrN_3O$ 372.0711 + found 372.0707 [M + H].

1-Butyl-1*H*-indazole-3-carboxylic acid to *N*-(3-bromophenyl)-1-butyl-1*H*-indazole-3-carboxamide (4). Appearance: brown solid melting point = 96–99 °C, yield = 78.4%, weight = 200 mg). ^{1}H NMR [400 MHz, CDCl$_3$]: δ 8.78 (s, 1H), 8.32 (d, J = 8.40 Hz, 1H), 7.95 (d, J = 1.60 Hz, 1H), 7.60–7.59 (m, 1H), 7.37–7.36 (m, 2H), 7.16 (t, J = 7.20 Hz, 2H), 4.34 (t, J = 7.20 Hz, 2H), 1.87 (q, J = 7.60 Hz, 2H), 1.34–1.32 (m, 2H), 0.89 (t, J = 7.20 Hz, 3H). ^{13}C NMR [100 MHz, CDCl$_3$]: δ 160.51, 141.11, 139.38, 136.73, 126.99, 126.83, 123.03, 122.94, 122.73, 122.44, 118.03, 109.48, 49.38, 31.38, 20.07, 13.66. IR STRECHING (cm^{-1}): 3272 (N–H), 1655 (C=O). HRMS (ESI) m/z: [M + H] calculated $C_{18}H_{18}BrN_3O$ 372.0711 + found 372.0707 [M + H].

1-Butyl-*N*-(4-methyl-[1,1-biphenyl]-4-yl)-1*H*-indazole-3-carboxamide (6a). Appearance: off white solid, yield = 94%, weight = 145 mg, melting point = 94–97 °C, (eluent = 15% ethyl acetate/hexane). ^{1}H NMR [400 MHz, CDCl$_3$]: δ 8.83 (s, 1H), 8.37 (d, J = 8.00 Hz, 1H), 7.75 (d, J = 8.40 Hz, 2H), 7.52 (d, J = 8.80 Hz, 2H), 7.43 (t, J = 8.40 Hz, 2H), 7.36 (t, J = 2.00 Hz, 2H), 7.17 (t, J = 5.60 Hz, 2H), 4.35 (t, J = 7.20 Hz, 3H), 2.31 (s, 2H), 1.88 (q, J = 7.60 Hz, 2H), 1.26–1.27 (m, 2H), 0.90 (t, J = 7.20 Hz, 3H). ^{13}C NMR [100 MHz, CDCl$_3$]: δ 160.54, 141.11, 137.78, 137.16, 137.14, 136.79, 136.71, 129.51, 127.45, 126.91, 126.68, 123.00, 122.91, 122.88, 119, 109.41, 49.34, 31.85, 21.11, 20.09, 13.68. DEPT-135 NMR [100 MHz, CDCl$_3$]: δ 129.51, 127.45, 126.91, 122.91, 122.88, 119.94, 109.42, 49.35, 31.85, 21.11, 20.09, 13.69. FT-IR (cm^{-1}): 3358 (N–H), 1659 (C=O). HRMS (ESI) m/z: [M + H] calculated $C_{25}H_{25}N_3O$ 384.2076 + found 384.2078 [M + H].

1-Butyl-*N*-(4-(trifluoromethyl)-[1,1-biphenyl]-4-yl)-1*H*-indazole-3-carboxamide (6b). Appearance: off white solid, yield = 93.7%, weight = 165 mg, melting point = 101–105 °C, (eluent = 15% ethyl acetate/hexane), ^{1}H NMR [400 MHz, CDCl$_3$]: δ 8.88 (s, 1H), 8.37 (d, J = 8.00 Hz, 1H), 7.80 (d, J = 8.80 Hz, 2H), 7.59–7.61 (m, 4H), 7.55 (d, J = 8.40 Hz, 2H), 7.37 (t, J = 1.60 Hz, 2H), 4.36 (t, J = 7.20 Hz, 2H), 1.89 (q, J = 7.20 Hz, 2H), 1.26–1.28 (m, 2H), 0.90 (t, J = 7.20 Hz, 3H). ^{13}C NMR [100 MHz, CDCl$_3$]: δ 160.60, 144.11, 141.12, 138.29, 136.98, 135.06, 129.18, 128.85, 127.85, 127.02, 126.98, 125.70, 122.98, 122.83, 120.00, 109.46, 49.38, 31.84, 20.08, 13.67. DEPT-135 NMR [100 MHz, CDCl$_3$]: δ 127.085, 127.02, 126.98, 125.70, 122.98, 120.00, 109.46, 109.46, 49.38, 31.84, 20.08, 13.67. FT-IR (cm^{-1}): 3351 (N–H), 1664 (C=O). HRMS (ESI) m/z: [M + H] calculated $C_{25}H_{22}F_3N_3O$ 438.1793 + found 438.1794 [M + H].

***N*-([1,1-Biphenyl]-4-yl)-1-butyl-1*H*-indazole-3-carboxamide (6c).** Appearance: off white solid, yield = 87%, weight = 130 mg, melting point = 83–88 °C, (eluent = 10% ethyl acetate/hexane), ^{1}H NMR [400 MHz, CDCl$_3$]: δ 8.85 (s, 1H), 8.37 (d, J = 8.00 Hz, 1H), 7.77 (d, J = 8.40 Hz, 2H), 7.53–7.54 (m, 4H), 7.34–7.36 (m, 4H), 4.35 (t, J = 6.80 Hz, 2H), 1.89 (q, J = 7.60 Hz, 2H), 1.36–1.34 (m, 2H), 0.90 (t, J = 7.20 Hz, 3H). ^{13}C NMR [100 MHz, CDCl$_3$]: δ 160.55, 141.12, 140.66, 137.43, 137.12, 136.75, 128.78, 127.03, 126.92, 126.85, 123.01, 122.91, 119.94, 109.41, 49.35, 31.84, 20.08, 13.67. DEPT-135 NMR [100 MHz, CDCl$_3$]: δ 128.78, 127.67, 127.03, 126.86, 122.91, 122.89 119.93, 109.41, 49.35, 31.85, 20.09, 13.68. FT-IR (cm^{-1}): N–H (3363), C=O (1660). HRMS (ESI) m/z: [M + H] calculated $C_{24}H_{22}N_3O$ 370.1919 + found 370.1924 [M + H].

1-Butyl-*N*-(4-(hydroxymethyl)-[1,1-biphenyl]-4-yl)-1*H*-indazole-3-carboxamide (6d). Appearance: off white solid (yield = 89.7%, weight = 145 mg, melting point = 81–86 °C, (eluent = 25% ethyl acetate/hexane), ^{1}H NMR [400 MHz, CDCl$_3$]: δ 8.86 (s, 1H), 8.37 (d, J = 7.60 Hz, 1H), 7.76 (d, J = 7.20 Hz, 2H), 7.53 (s, 3H), 7.46 (d, J = 6.40 Hz, 1H), 7.36 (d, J = 9.20 Hz, 3H), 7.25 (d, J = 5.60 Hz, 2H), 4.69 (s, 2H), 4.35 (s, 2H), 1.88 (s, 2H), 1.31 (d, J = 6.80 Hz, 2H), 0.90 (t, J = 6.80 Hz, 3H). ^{13}C NMR [100 MHz, CDCl$_3$]: δ 160.59, 141.50, 141.09, 137.48, 137.06, 136.46, 136.46, 129.02, 127.66, 126.94, 126.10, 125.64, 125.42, 122.99, 122.93, 122.87, 119.94, 109.44, 65.37, 49.35, 31.85, 20.08, 13.69. DEPT-135 NMR [100 MHz, CDCl$_3$]: δ 129.02, 127.66, 126.94, 126.10, 125.65, 125.42, 122.93, 122.86, 119.94, 109.44, 65.37, 49.35, 31.85, 20.09, 13.69. FT-IR (cm^{-1}): 3403 (OH), 3250 (N–H), 1645 (C=O). HRMS (ESI) m/z: [M + H] calculated $C_{25}H_{25}N_3O_2$ 400.2025 + found 400.2037 [M + H].

1-Butyl-*N*-(4-formyl-[1,1-biphenyl]-4-yl)-1*H*-indazole-3-carboxamide (6e). Appearance: off white solid, yield = 87.5%, weight = 140 mg, melting point = 93–97 °C, (eluent = 25% ethyl acetate/hexane), ^{1}H NMR [400 MHz, CDCl$_3$]: δ 10.01 (s, 1H), 8.89 (s, 1H), 8.37 (d, J = 8.00 Hz, 1H), 8.03 (s, 1H), 7.75–7.77 (m, 4H), 7.58 (d, J = 8.64 Hz, 2H), 7.52 (t, J = 8.00 Hz, 1H), 7.37–7.38 (m, 2H), 4.36 (t, J = 7.20 Hz, 2H), 1.89 (q, J = 7.20 Hz, 2H), 1.26–1.28 (m, 2H), 0.00 (t, J = 7.20 Hz, 3H). ^{13}C NMR [100 MHz, CDCl$_3$]: δ 192.45, 160.61, 141.56, 138.12, 136.98, 136.94, 135.04, 129.52, 128.38, 127.81, 127.70, 126.97, 122.97, 122.83, 122.05, 109.46, 49.38, 31.84, 20.08, 13.67. DEPT-135 NMR [100 MHz, CDCl$_3$]: δ 132.74, 129.52, 128.39, 127.81, 127.70, 126.97, 122.97, 122.82, 120.05, 109.46, 49.38, 31.84, 20.08, 13.68. FT-IR (cm^{-1}): 2955 (CHO), 3301 (N–H), 1693 (C=O). HRMS (ESI) m/z: [M + H] calculated $C_{25}H_{23}N_3O_2$ 398.1868 + found 398.1868 [M + H].

1-Butyl-*N*-(3-fluoro-4-methoxy-[1,1-biphenyl]-4-yl)-1*H*-indazole-3-carboxamide (6f). Appearance: off white solid, yield = 71.4%, weight = 120 mg, melting point = 80–85 °C, (eluent = 15% ethyl acetate/hexane), ^{1}H NMR [400 MHz, $CDCl_3$]: δ 8.84 (s, 1H), 8.37 (d, J = 8.00 Hz, 1H), 7.76 (d, J = 8.00 Hz, 2H), 7.48 (d, J = 7.60 Hz, 2H), 7.39 (s, 2H), 7.19–7.26 (m, 4H), 6.95 (t, J = 8.00 Hz, 1H), 4.37 (t, J = 6.80 Hz, 2H), 3.86 (s, 3H), 1.90 (t, J = 7.20 Hz, 2H), 1.32 (q, J = 6.80 Hz, 2H), 0.912 (t, J = 6.80 Hz, 3H). ^{13}C NMR [100 MHz, $CDCl_3$]: δ 160.65, 141.11, 138.62, 137.04, 129.51, 127.20, 126.39, 122.97, 122.91, 122.85, 122.26, 119.98, 118.41, 117.92, 115.00, 114.81, 113.58, 109.43, 56.37, 49.36, 31.84, 20.08, 13.68. DEPT-135 NMR [100 MHz, $CDCl_3$]: δ 129.51, 127.20, 126.93, 122.91, 122.86, 122.26, 119.98, 118.41, 117.92, 115.00, 114.81, 113.56, 109.44, 56.37, 49.36, 31.85, 20.08, 13.68. FT-IR (cm^{-1}): 3380 (N–H), 2955 (–OCH_3), 1681 (C=O). HRMS (ESI) m/z: [M + H] calculated $C_{25}H_{24}FN_3O_2$ 418.1931 + found 418.1933 [M + H].

4-(1-Butyl-1*H*-indazole-3-carboxamido)-[1,1-biphenyl]-3-carboxylic acid (6g). Appearance: off white solid, yield = 71.8%, weight = 120 mg, melting point = 159–164 °C, (eluent = 30% ethyl acetate/hexane) ^{1}H NMR [400 MHz, DMSO-d_6]: δ 10.39 (s, 1H), 8.26 (d, J = −8.40 Hz, 1H), 8.22 (s, 1H), 8.05 (d, J = 8.40 Hz, 2H), 7.92 (t, J = 8.40 Hz, 2H), 7.84 (d, J = 8.40 Hz, 1H), 7.73 (d, J = 8.80 Hz, 2H), 7.60 (t, J = 7.60 Hz, 1H), 7.51 (t, J = 8.00 Hz, 1H), 7.34 (t, J = 7.60 Hz, 1H), 4.57 (t, J = 7.20 Hz, 2H), 0.00 (q, J = 7.20 Hz, 2H), 1.27–1.28 (m, 2H), 0.92 (t, J = 7.60 Hz, 3H). ^{13}C NMR [100 MHz, $CDCl_3$]: δ 167.18, 161.14, 141.9, 140.54, 139.14, 137.37, 134.62, 132.00, 131.14, 129.77, 128.32, 127.39, 127.24, 123.16, 122.91, 122.22, 121.22, 111.02, 49.11, 31.99, 19.93, 14.02. DEPT-135 NMR [100 MHz, $CDCl_3$]: δ 131.14, 129.77, 128.33, 127.39, 127.36, 127.25, 123.17, 122.22, 121.22, 111.03, 49.11, 31.99, 19.93, 14.02. FT-IR (cm^{-1}): 3281 (N–H), 1715 (C=O). HRMS (ESI) m/z: [M + H] calculated $C_{25}H_{23}N_3O_3$ 414.1817 + found 414.1818 [M + H].

1-Butyl-*N*-(4-(methylsulfonyl)-[1,1-biphenylyl]-4-yl)-1*H*-indazole-3-carboxamide (6h). Appearance: off white solid, yield = 94.4%, weight = 170 mg, melting point = 79–84 °C, (eluent = 15% ethyl acetate/hexane), ^{1}H NMR [400 MHz, $CDCl_3$]: δ 8.98 (s, 1H), 8.44 (d, J = −8.00 Hz, 1H), 8.00 (d, J = 8.00 Hz, 2H), 7.91 (d, J = 8.40 Hz, 2H), 7.79 (d, J = 8.40 Hz, 2H), 7.65 (d, J = 8.40 Hz, 2H), 7.47 (d, J = 4.80 Hz, 2H), 7.32–7.32 (m, 1H), 4.45 (t, J = 7.20 Hz, 2H), 3.10 (s, 3H), 1.98 (q, J = 7.20 Hz, 2H), 1.35–1.37 (m, 2H), 0.99 (t, J = 7.20 Hz, 3H). ^{13}C NMR [100 MHz, $CDCl_3$]: δ 160.61, 1466.10, 141.15, 138.79, 138.75, 136.93, 134.33, 128.02, 127.94, 127.54, 127.01, 123.02, 122.99, 122.80, 120.06, 109.47, 49.40, 44.67, 31.83, 20.07, 13.65. DEPT-135 NMR [100 MHz, $CDCl_3$]: δ 128.28, 126.96, 126.86, 126.46, 125.97, 122.00, 121.73, 119.91, 119.01, 116.73, 48.32, 43.53, 30.78, 28.66, 19.02, 12.63. FT-IR (cm^{-1}): 3075 (N–H), 1676 (C=O). HRMS (ESI) m/z: [M + H] calculated $C_{25}H_{23}N_3O_3S$ 448.1695 + found 448.1697 [M + H].

1-Butyl-*N*-(2-nitro[1,1-biphenyl]-4-1*H*-indazole-3-carboxamide) (6i). Appearance: off white solid, yield = 59.8%, weight = 100 mg, melting point = 88–94 °C, (eluent = 15% ethyl acetate/hexane), ^{1}H NMR [400 MHz, $CDCl_3$]: δ 8.86 (s, 1H), 8.37 (d, J = 8.00 Hz, 1H), 7.77 (d, J = 7.60 Hz, 3H), 7.54 (t, J = 7.60 Hz, 1H), 7.40 (d, J = 9.20 Hz, 4H), 7.28 (s, 1H), 4.37 (t, J = 7.20 Hz, 2H), 1.90 (q, J = 7.20 Hz, 2H), 1.30 (d, J = 35.60 Hz, 2H), 0.91 (t, J = 7.20 Hz, 3H). ^{13}C NMR [100 MHz, $CDCl_3$]: δ 160.57, 149.36, 141.14, 138.27, 137, 135.87, 132.69, 132.24, 132, 128.7, 126.94, 124.1, 123, 122.93, 122.87, 119.76, 109.43, 49.36, 31.81, 20.06, 13.64. DEPT-135 NMR [100 MHz, $CDCl_3$]: δ 132.24, 132, 128.7, 127.97, 126.94, 124.1, 122.93, 122.87, 119.76, 109.43, 49.36, 31.81, 20.06, 13.64. FT-IR (cm^{-1}): 3390 (N–H), 1671 (C=O), 1521 (NO_2). HRMS (ESI) m/z: [M + H] calculated $C_{25}H_{22}N_4O_3$ 415.1770 + found 415.1773 [M + H].

1-Butyl-*N*-(3-fluoro-4-methoxy-[1,1-biphenyl]-3-yl)-1*H*-indazole-3-carboxamide (7a). Appearance: off white solid, yield = 88.8%, weight = 150 mg, melting point = 96–100 °C, (eluent = 15% ethyl acetate/hexane), ^{1}H NMR [400 MHz, $CDCl_3$]: δ 8.86 (s, 1H), 8.37 (d, J = 8.00 Hz, 1H), 7.93 (s, 1H), 7.63 (d, J = 8.00 Hz, 1H), 7.30–7.31 (m, 5H), 7.18–7.21 (m, 2H), 6.95 (t, J = 8.80 Hz, 1H), 4.36 (t, J = 6.80 Hz, 2H), 3.86 (s, 3H), 1.90 (q, J = 7.20 Hz, 2H), 1.27–1.29 (m, 2H), 0.904 (t, J = 7.60 Hz, 3H). ^{13}C NMR [100 MHz, $CDCl_3$]: δ 160.66, 153.77, 147.24, 141.11, 140.66, 138.62, 137.35, 137.04, 129.51, 127.19, 126.93,122.97, 122.83, 122.26, 119.99, 118.42, 117.92, 114.99, 109.44, 56.37, 49.36, 31.84, 20.08, 13.67. DEPT-135 NMR [100 MHz, $CDCl_3$]: δ 129.51, 127.20, 126.93, 122.91, 122.83, 122.26, 119.99, 118.42, 117.92, 114.99, 114.80, 113.59, 113.57, 109.44 56.37, 49.36, 31.85, 20.08, 13.68. FT-IR (cm^{-1}): 3277 (N–H), 2767 (OCH_3), 1664 (C=O). HRMS (ESI) m/z: [M + H] calculated $C_{25}H_{24}FN_3O_2$ 418.1931+ found 418.1931 [M + H].

1-Butyl-*N*-(4-(trifluoromethyl)-[1,1-biphenyl]-3-yl)-1*H*-indazole-3-carboxamide (7b). Appearance: off white solid, yield = 73.8%, weight = 130 mg, melting point = 66–70 °C, (eluent = 15% ethyl acetate/hexane), ^{1}H NMR [400 MHz, $CDCl_3$]: δ 8.89 (s, 1H), 8.37 (d, J = 8.00 Hz, 1H), 8.05 (s, 1H), 7.61–7.64 (m, 5H), 7.38–7.39 (m, 3H), 7.18 (d, J = 3.60 Hz, 1H), 4.37 (t, J = 6.80 Hz, 2H), 1.90 (q, J = 7.20 Hz, 2H), 1.27–1.29 (m, 2H), 0.91 (t, J = 7.60 Hz, 3H). ^{13}C NMR [100 MHz, $CDCl_3$]: δ 160.69, 144.40, 141.14, 140.71, 138.77, 136.99, 129.64, 127.58, 126.97, 125.69, 125.65, 122.97, 122.77, 119.30, 118.50, 109.45, 49.38, 31.84, 20.08, 13.66. DEPT-135 NMR [100 MHz, $CDCl_3$]: δ 129.64, 127.58, 126.97, 125.69, 122.97, 122.83, 122.78, 119.30, 118.50, 109.45, 49.38, 31.84, 20.08, 13.66. FT-IR (cm^{-1}): 3289 (N–H), 1668 (C=O). HRMS (ESI) m/z: [M + H] calculated $C_{25}H_{22}F_3N_3O$ 438.1793 + found 438.1795 [M + H].

1-Butyl-*N*-(4-methyl-[1,1-biphenyl]-3-yl)-1*H*-indazole-3-carboxamide (7c). Appearance: off white solid, yield = 90.9%, weight = 140 mg, melting point = 107–110 °C, (eluent = 15% ethyl acetate/hexane), ^{1}H NMR [400 MHz, $CDCl_3$]: δ 8.86 (s, 1H), 8.38 (d, J = 8.00 Hz, 1H), 7.92 (s, 1H), 7.68 (d, J = 8.00 Hz, 1H), 7.49 (d, J = 8.00 Hz, 2H), 7.34–7.36 (m, 3H), 7.29 (s, 1H), 7.18 (t, J = 4.40 Hz, 2H), 4.37 (t, J = 7.20 Hz, 2H), 2.33 (s, 3H), 1.90 (q, J = 7.60 Hz, 2H), 1.27–1.29 (m, 2H), 0.91 (t, J = 7.60 Hz, 3H). ^{13}C NMR [100 MHz, $CDCl_3$]: δ 160.61, 142.11, 141.11, 138.50, 137.94, 137.24, 137.15, 129.45, 129.39, 127.10, 126.90, 122.99, 122.91, 122.85, 122.57, 118.27, 118.17, 109.40, 49.34, 31.85, 21.14, 20.09, 13.68. DEPT-135 NMR [100 MHz, $CDCl_3$]: δ 129.46, 129.40, 127.10, 126.90, 122.91, 122.86, 122.57, 118.27, 118.17, 109.40, 49.34, 31.85, 21.14, 20.09, 13.68. FT-IR (cm^{-1}): 3289 (N–H), 1668 (C=O). HRMS (ESI) m/z: [M + H] calculated $C_{25}H_{25}N_3O$ 384.2076 + found 384.2080 [M + H].

***N*-([1,1-Biphenyl]-3-yl)-1-butyl-1*H*-indazole-3-carboxamide (7d).** Appearance: off white solid, yield = 67.1%, weight = 100 mg, melting point = 65–68 °C, (eluent = 10% ethyl acetate/hexane), ^{1}H NMR [400 MHz, $CDCl_3$]: δ 8.94 (s, 1H), 8.45 (d, J = 6.80 Hz, 1H), 8.02 (s, 1H), 7.76 (d, J = 6.00 Hz, 1H), 7.66 (d, J = 5.60 Hz, 2H), 7.33–7.36 (m, 8H), 4.43 (s, 2H), 1.97 (s, 2H), 1.38 (d, J = 6.00 Hz, 2H), 0.97 (s, 3H). ^{13}C NMR [100 MHz, $CDCl_3$]: δ 160.63, 142.21, 141.12, 140.86, 138.55, 137.12, 129.44, 128.74, 127.46, 127.29, 123.00, 122.90, 122.88, 118.52, 118.41, 109.42, 49.35, 31.85, 20.09, 13.68. DEPT-135 NMR [100 MHz, $CDCl_3$]: δ 129.44, 128.74, 127.29, 126.91, 122.88, 122.75, 118.52, 118.41, 109.42, 49.35, 31.85, 20.09, 13.68. FT-IR (cm^{-1}): 3014 (N–H), 1670 (C=O). HRMS (ESI) m/z: [M + H] calculated $C_{24}H_{24}N_3O$ 370.1919 + found 370.1920 [M + H].

1-Butyl-*N*-(4-formyl-[1,1-biphenyl]-3-yl)-1*H*-indazole-3-carboxamide (7e). Appearance: off white solid, yield = 74.6%, weight = 120 mg, melting point = 67–72 °C, (eluent = 25% ethyl acetate/hexane) ^{1}H NMR [400 MHz, $CDCl_3$]: δ 10.10 (s, 1H), 9.00 (s, 1H), 8.44 (d, J = 6.40 Hz, 1H), 8.13 (d, J = 14.40 Hz, 2H), 7.76–7.78 (m, 3H), 7.61 (s, 1H), 7.26–7.33 (m, 5H), 4.45 (s, 2H), 1.98 (s, 2H), 1.39 (d, J = 5.20 Hz, 2H), 0.98 (s, 3H). ^{13}C NMR [100 MHz, $CDCl_3$]: δ 192.47, 160.76, 141.82, 140.66, 138.73, 136.93, 136.87, 133.29, 129.71, 129.51, 128.72, 128.44, 126.98, 122.96, 122.78, 122.72, 119.21, 118.40, 109.48, 49.40, 31.85, 20.09, 13.68. DEPT-135 NMR [100 MHz, $CDCl_3$]: δ 133.28, 129.71, 129.51, 128.72, 128.44, 126.98, 122.99, 122.71, 119.21, 118.39, 109.48, 49.40, 31.85, 20.09, 13.68. FT-IR (cm^{-1}): 3257 (N–H), 2952 (CHO), 1690 (C=O). HRMS (ESI) m/z: [M + H] calculated $C_{25}H_{23}N_3O_2$ 398.1868 + found 398.1873 [M + H].

1-Butyl-*N*-(4-(hydroxymethyl)-[1,1-biphenyl]-3-yl)-1*H*-indazole-3-carboxamide (7f). Appearance: off white solid, yield = 74.3%, weight = 120 mg, melting point = 77–82 °C, (eluent = 25% ethyl acetate/hexane), ^{1}H NMR [400 MHz, $CDCl_3$]: δ 8.97 (s, 1H), 8.43 (d, J = 7.60 Hz, 1H), 8.01 (s, 1H), 7.74 (d, J = 7.20 Hz, 1H), 7.64 (s, 1H), 7.57 (d, J = 7.60 Hz, 1H), 7.42–7.44 (m, 4H), 7.26–7.31 (m, 3H), 4.76 (s, 2H), 4.58 (s, 1H), 4.43 (t, J = 6.40 Hz, 2H), 1.95–1.97 (m, 2H), 1.36–1.37 (m, 2H), 0.97 (t, J = 7.20 Hz, 3H). ^{13}C NMR [100 MHz, $CDCl_3$]: δ 160.71, 141.94, 141.39, 141.12, 138.47, 137.03, 129.76, 129.46, 128.99, 126.95, 126.57, 126.10, 125.87, 122.97, 122.94, 122.84, 122.81, 118.67, 118.44, 114.65, 113.84, 109.44, 49.37, 31.85, 20.08, 13.68. DEPT-135 NMR [100 MHz, $CDCl_3$]: δ 129.76, 129.47, 128.99, 126.95, 126.57, 126.10, 125.87, 122.94, 122.84, 122.81, 118.82, 118.67, 118.44, 114.66, 113.84, 109.44, 65.04, 49.38, 31.85, 20.09, 13.68. FT-IR (cm^{-1}): 3383 (O–H), 1663 (C=O). HRMS (ESI) m/z: [M + H] calculated $C_{25}H_{25}N_3O_2$ 400.2025 + found 400.2027 [M + H].

3-(1-Butyl-1*H*-indazole-3-carboxamido)-[1,1-biphenyl]-3-carboxylic acid (7g). Appearance: off white solid, yield = 89.8%, weight = 150 mg, melting point = 145–148 °C, (eluent = 30% ethyl acetate/hexane), ^{1}H NMR [400 MHz, $CDCl_3$]: δ 8.95 (s, 1H), 8.38 (d, J = 8.00 Hz, 1H), 8.33 (s, 1H), 8.04 (d, J = 7.60 Hz, 1H), 7.95 (s, 1H), 7.84 (d, J = 7.60 Hz, 1H), 7.78 (d, J = 8.00 Hz, 1H), 7.48 (t, J = 7.60 Hz, 1H), 7.32–7.34 (m, 4H), 4.37 (t, J = 7.20 Hz, 2H), 1.90 (q, J = 7.20 Hz, 2H), 1.27–1.29 (m, 2H), 0.90 (t, J = 7.20 Hz, 3H). ^{13}C NMR [100 MHz, $CDCl_3$]: δ 175.23, 160.68, 141.29, 141.12, 140.91, 138.71, 132.56, 129.67, 129.17, 129.00, 128.90, 126.94, 122.99, 122.93, 122.88, 122.75, 119.08, 118.37, 109.43, 49.38, 31.86, 20.09, 13.68. DEPT-135 NMR [100 MHz, $CDCl_3$]: δ 135.56, 129.67, 129.17, 129.00, 128.89, 126.95, 122.94, 122.88, 122.76, 119.08, 118.37, 109.43, 49.38, 31.86, 20.09, 13.68. FT-IR (cm^{-1}): 3281 (N–H), 1715 (C=O). HRMS (ESI) m/z: [M + H] calculated $C_{25}H_{23}N_3O_3$ 414.1817 + found 414.1818 [M + H].

1-Butyl-*N*-(4-(methylsulfonyl)-[1,1-biphenyl]-3-yl)-1*H*-indazole-3-carboxamide (7h). Appearance: off white solid, yield = 94.4%, weight = 170 mg, melting point = 110–106 °C, (eluent = 25% ethyl acetate/hexane), ^{1}H NMR [400 MHz, $CDCl_3$]: δ 8.91 (s, 1H), 8.36 (d, J = 8.00 Hz, 1H), 8.12 (d, J = Hz, 1H), 7.94 (d, J = 8.40 Hz, 2H), 7.77 (d, J = 8.00 Hz, 2H), 7.65 (d, J = 7.60 Hz, 1H), 7.38–7.40 (m, 3H), 7.30 (d, J = 7.60 Hz, 1H), 7.19 (s, 1H), 4.38 (t, J = 7.20 Hz, 2H), 3.03 (s, 3H), 0.91 (q, J = 7.20 Hz, 2H), 1.27–1.29 (m, 2H), 0.91 (t, J = 7.20 Hz, 3H). ^{13}C NMR [100 MHz, $CDCl_3$]: δ 159.70, 145.41, 140.13, 139.08, 138.27, 137.88, 135.90, 128.73, 127.16, 125.98, 121.99, 121.96, 121.82, 121.76, 118.71, 108.45, 48.37, 43.65, 30.81, 19.05, 12.63. DEPT-135 NMR [100 MHz, $CDCl_3$]: δ 128.72, 127.15, 126.85, 125.97, 121.98, 121.81, 121.72, 118.68, 117.57, 108.46, 48.36, 43.64, 30.81, 19.04, 12.64. FT-IR (cm^{-1}): N–H (3336), 1669 (C=O). HRMS (ESI) m/z: [M + H] calculated $C_{25}H_{25}N_3O_3S$ 448.1695 + found 448.1876 [M + H].

1-Butyl-*N*-(2-nitro-[1,1-biphenyl]-3-yl)-1*H*-indazole-3-carboxamide (7i). Appearance: off white solid, yield = 71.8%, weight = 120 mg, melting point = 99–104 °C, (eluent = 15% ethyl acetate/hexane), ^{1}H NMR [400 MHz, $CDCl_3$]: δ 8.93 (s, 1H), 8.42 (d, J = 8.00 Hz, 1H), 7.89 (d, J = 8.00 Hz, 1H), 7.80 (d, J = 9.20 Hz, 1H), 7.62 (d, J = 7.20 Hz, 1H), 7.52 (d, J = 6.00 Hz, 1H), 7.43–7.44 (m, 3H), 7.32 (t, J = 6.00 Hz, 1H), 7.26 (s, 1H), 7.07 (d, J = 7.60 Hz, 1H), 4.44 (t, J = 7.20 Hz, 2H), 0.00 (q, J = 7.60 Hz, 2H), 1.33–1.35 (m, 2H), 0.98 (t, J = 7.20 Hz, 3H). ^{13}C NMR [100 MHz, $CDCl_3$]: δ 160.61, 149.20, 141.11, 138.43, 138.39, 136.92, 136.16, 132.35, 129.36, 128.30, 126.91, 124.10, 123.39, 122.96, 122.82, 119.37, 119.12, 109.44, 49.36, 31.82, 20.07, 13.67. DEPT-135 NMR [100 MHz, $CDCl_3$]: δ 132.35, 132.15, 129.37, 128.30, 126.92, 124.11, 123.39, 122.92, 122.82, 119.37, 119.12, 109.14. FT-IR (cm^{-1}): N–H (3384), C=O (1676), NO_2 (1524). HRMS (ESI) m/z: [M + H] calculated $C_{25}H_{22}N_3O_3$ 415.1770 + found 415.1771 [M + H].

Data availability

Detailed experimental procedures and characterization data for all novel compounds such as ^{1}H and ^{13}C NMR, Dept-135, COSY, HSQC, IR, and HRMS spectra are submitted as ESI.† The above content also included in the appropriate section of the manuscript.

Author contributions

The corresponding author Vijayaparthasarathi Vijayakumar has designed and executed the work, while the first author Bandaru Gopi has synthesized and characterized the target molecules and carried out the studies.

Conflicts of interest

No conflict of interest.

Acknowledgements

The VIT University administration in Vellore, India, is acknowledged by the authors for the seed grant (SG20230086) and for providing research facilities; and SIF-Chemistry at VIT University for providing NMR facilities. We sincerely thank Dr S. Sarveswari for her perceptive feedback and valuable insights on how to wrap up the research. The author acknowledges Ms. Rebecca Susan Philip's suggestion to finish the assignment.

References

1 Z. Yang, J. T. Yu and C. Pan, *Org. Biomol. Chem.*, 2022, **20**, 7746–7764.
2 L. Zhang, H. Yan, Y. Fan, X. Luo, Y. Pan, Y. Liu, Y. Cai and Q. Xia, *J. Org. Chem.*, 2023, **88**, 5731–5744.
3 T. Y. Wu, S. Dhole, M. Selvaraju and C. M. Sun, *ACS Comb. Sci.*, 2018, **20**, 156–163.
4 H. Zhang, Z. Ye, N. Chen, Z. Chen and F. Zhang, *Green Chem.*, 2022, **24**, 1463–1468.
5 W. Wei, Z. Liu, X. Wu, C. Gan, X. Su, H. Liu, H. Que, Q. Zhang, Q. Xue, L. Yue, L. Yu and T. Ye, *RSC Adv.*, 2021, **11**, 15675–15687.
6 S. Miyamoto, S. Kakutani, Y. Sato, A. Hanashi, Y. Kinoshita and A. Ishikawa, *Jpn. J. Clin. Oncol.*, 2018, **48**, 503–513.
7 A. R. He, R. B. Cohen, C. S. Denlinger, A. Sama, A. Birnbaum, J. Hwang, T. Sato, N. Lewis, M. Mynderse, M. Niland, J. Giles, J. Wallin, B. Moser, W. Zhang, R. Walgren and E. R. Plimack, *Oncologist*, 2019, **24**, e930–e942.
8 Z. T. Al-Salama and S. J. Keam, *Drugs*, 2019, **79**, 1477–1483.
9 S. Puri and K. Juvale, *J. Mol. Struct.*, 2022, **1269**, 133727.
10 H. Sung, J. Ferlay, R. L. Siegel, M. Laversanne, I. Soerjomataram, A. Jemal and F. Bray, *Ca-Cancer J. Clin.*, 2021, **71**, 209–249.
11 L. Bukavina, K. Bensalah, F. Bray, M. Carlo, B. Challacombe, J. A. Karam, W. Kassouf, T. Mitchell, R. Montironi, T. O'Brien, V. Panebianco, G. Scelo, B. Shuch, H. van Poppel, C. D. Blosser and S. P. Psutka, *Eur. Urol.*, 2022, **82**, 529–542.
12 Y. Wan, S. He, W. Li and Z. Tang, *Anticancer Agents Med. Chem.*, 2018, **18**, 1228–1234.
13 M. R. Tammana, V. Vijayakumar and S. Sarveswari, *J. Indian Chem. Soc.*, 2024, 101168.
14 H. J. Zhang, G. T. Tan, V. D. Hoang, N. Van Hung, N. M. Cuong, D. D. Soejarto, J. M. Pezzuto and H. H. S. Fong, *J. Nat. Prod.*, 2003, **66**, 263–268.
15 B. Gopi and V. Vijayakumar, *RSC Adv.*, 2024, **14**(19), 13218–13226.
16 D. R. Kerzare, S. S. Menghani and P. B. Khedekar, *Indian J. Pharm. Educ. Res.*, 2018, **52**, 110–121.
17 B. Ko, Y. Jang, M. H. Kim, T. T. Lam, H. K. Seo, P. Jeong, M. Choi, K. W. Kang, S. D. Lee, J. H. Park, M. Kim, S. Y. Han and Y. C. Kim, *Eur. J. Med. Chem.*, 2023, **262**, 115860.
18 J. M. Honnanayakanavar, O. Obulesu and S. Suresh, *Org. Biomol. Chem.*, 2022, **20**, 2993–3028.
19 Y. H. Khan, S. Qasim, A. M. Uttra, N. H. Alotaibi, A. S. Alanazi, A. I. Alzarea, A. D. Alatawi and T. Hussain Mallhi, *Life Sci.*, 2023, **324**, 121742.
20 X. P. Kang, W. Lian, L. Xu, J. Wang, H. Jia, B. Zhang, A. L. Liu and G. H. Du, *RSC Adv.*, 2018, **8**, 5286–5297.
21 R. Rafique, K. M. Khan, K. Arshia, S. Chigurupati, A. Wadood, A. U. Rehman, A. Karunanidhi, S. Hameed, M. Taha and M. al-Rashida, *Bioorg. Chem.*, 2020, **94**, 103195.
22 S. Bhattacharjee, S. Laru and A. Hajra, *Org. Biomol. Chem.*, 2022, **20**, 8893–8897.
23 Q. Pan, Y. Wu, A. Zheng, X. Wang, X. Li, W. Wang, M. Gao, Z. Bibi, S. Chaudhary and Y. Sun, *Molecules*, 2023, **28**, 7190.
24 J. Yu, A. Zheng, L. Jin, Y. Wu, Q. Pan, X. Wang, X. Li, W. Wang, M. Gao and Y. Sun, *Appl. Sci.*, 2023, **13**, 4095.
25 V. Hemalatha and V. Vijayakumar, *Inorg. Chem. Commun.*, 2022, **144**, 109894.
26 M. S. Sunitha and S. Sarveswari, *Inorg. Chim. Acta*, 2024, **562**, 121893.
27 M. S. Sunitha and S. Sarveswari, *Inorg. Chem. Commun.*, 2024, **160**, 111973.
28 R. H. Waghchaure and V. A. Adole, *J. Mol. Struct.*, 2024, **1296**, 136724.
29 T. Uelisson da Silva, E. Tomaz da Silva, K. de Carvalho Pougy, C. Henrique da Silva Lima and S. de Paula Machado, *Inorg. Chem. Commun.*, 2022, **135**, 109120.
30 C. Kucuk, S. Celik, S. Yurdakul, E. Cotelı and B. Erdem, *Polyhedron*, 2023, (241), 116469.
31 J. K. Ojha, G. Ramesh and B. V. Reddy, *Chem. Phys. Impact*, 2023, (7), 100280.
32 M. A. Mumit, T. K. Pal, M. A. Alam, M. A. A. A. A. Islam, S. Paul and M. C. Sheikh, *J. Mol. Struct.*, 2020, **1220**, 128715.
33 A. Jumabaev, U. Holikulov, H. Hushvaktov, N. ISSAOUI and A. Absanov, *J. Mol. Liq.*, 2023, **377**, 121552.
34 V. Hemalatha and V. Vijayakumar, *J. Mol. Struct.*, 2024, **1311**, 138322.
35 S. S. Bushra, K. M. Khan, N. Ullah, M. Mahdavi, M. A. Faramarzi, B. Larijani, U. Salar, R. Rafique, M. Taha and S. Perveen, *J. Mol. Struct.*, 2021, **1242**, 130826.
36 D. Veeranna, L. Ramdas, G. Ravi, S. Bujji, V. Thumma and J. Ramchander, *ChemistrySelect*, 2022, e202201758.
37 M. Adib, F. Peytam, M. Rahmanian-Jazi, M. Mohammadi-Khanaposhtani, S. Mahernia, H. R. Bijanzadeh, M. Jahani, S. Imanparast, M. A. Faramarzi, M. Mahdavi and B. Larijani, *New J. Chem.*, 2018, **42**, 17268–17278.
38 V. H. Hoang, N. T. K. Trang, T. C. Minh, L. T. B. Long, T. H. Lan, N. T. Hue, L. Q. Tien, T. X. Nguyen, Y. T. K. Nguyen, H. Yoo and P. T. Tran, *Bioorg. Med. Chem.*, 2023, **90**, 117377.